

Second resonance of the Higgs field: more signals from the LHC experiments

Maurizio Consoli

INFN - Sezione di Catania, I-95129 Catania, Italy

maurizio.consoli@ct.infn.it

Leonardo Cosmai

INFN - Sezione di Bari, I-70126 Bari, Italy

leonardo.cosmai@ba.infn.it

Fabrizio Fabbri

INFN - Sezione di Bologna, I-40127 Bologna, Italy

fabrizio.fabbri@bo.infn.it

Received (Day Month Year)

Revised (Day Month Year)

Theoretical arguments and lattice simulations suggest that, beside the known resonance of mass $m_h = 125$ GeV, the Higgs field might exhibit a second resonance with a larger mass $(M_H)^{\text{theor}} = 690 \pm 10 \text{ (stat)} \pm 20 \text{ (sys)} \text{ GeV}$ which, however, would couple to longitudinal W's with the same typical strength as the low-mass state at 125 GeV and thus represent a relatively narrow resonance mainly produced at LHC by gluon-gluon fusion. By looking for some evidence in the LHC data, we argue that the existence of a new resonance in the predicted mass region finds support in two analyses by ATLAS (searching for heavy resonances decaying into final states with 4 charged leptons or $\gamma\gamma$ pairs) and in more recent CMS results (searching for heavy resonances decaying into a pair of $h(125)$ bosons or looking for $\gamma\gamma$ pairs produced in pp double-diffractive scattering). Since the correlation of these measurements is very small and since, having some definite theoretical prediction, local deviations from the pure background are not downgraded by the look-elsewhere effect, we emphasize the instability of the present situation that could probably be resolved by just adding two crucial, missing samples of RUN2 data.

PACS numbers: 11.30.Qc; 12.15.-y; 13.85.-t

1. Introduction

At present, the spectrum of the Higgs field is believed to consist of just a single narrow resonance of mass $m_h = 125$ GeV defined by the second derivative of the effective potential at its minimum. In a description of Spontaneous Symmetry Breaking (SSB) as a second-order phase transition, in the review of the Particle Data Group,¹ this point of view is well summarized into a scalar potential of the

form

$$V_{\text{PDG}}(\varphi) = -\frac{1}{2}m_{\text{PDG}}^2\varphi^2 + \frac{1}{4}\lambda_{\text{PDG}}\varphi^4 \quad (1)$$

By fixing $m_{\text{PDG}} \sim 88.8$ GeV and $\lambda_{\text{PDG}} \sim 0.13$, this has a minimum at $|\varphi| = \langle\Phi\rangle \sim 246$ GeV and a second derivative $V''_{\text{PDG}}(\langle\Phi\rangle) \equiv m_h^2 = (125 \text{ GeV})^2$. Notice that, here, one is adopting the identification $m_h^2 = V''_{\text{PDG}}(\langle\Phi\rangle) = |G^{-1}(p=0)|$ in terms of the inverse, zero-momentum propagator.

However, lattice simulations of cutoff Φ^4 in 4D²⁻⁴ support instead the view of SSB as a weak first-order phase transition. While in the presence of gauge bosons SSB can indeed be described, in perturbation theory, as a first-order transition, recovering this result in pure Φ^4 requires to replace standard perturbation theory with some alternative scheme. A scheme where SSB occurs when the quanta of the symmetric phase have a very small but still positive mass squared. Equivalently, a scheme where, as in the original Coleman-Weinberg (CW) 1-loop effective potential,⁵ the massless, classically scale-invariant theory is already found in the broken-symmetry phase. To exploit the implications of this different description of SSB, a crucial observation is that the CW potential admits two different readings. In a first perspective, where the genuine 1-loop contribution is understood as simply renormalizing the coupling λ in the classical potential, the 1-loop minimum disappears after re-summing the higher-order leading logarithmic terms. In a second perspective, recently emphasized in,⁶⁻⁸ the same CW potential can be read as the sum of the classical potential + the zero-point energy. Once interpreted in this way, it also acquires a non-perturbative meaning as the prototype⁹ of an *infinite* number of approximations, the Gaussian¹⁰ and post-gaussian calculations,^{11,12} which correspond to very different resummations of graphs but effectively reproduce the same basic structure of $V_{\text{eff}}(\varphi)$: some classical background + zero-point energy of a particle with some φ -dependent mass $M(\varphi)$. In these approximations, by defining $m_h^2 = V''_{\text{eff}}(\varphi)$ at the minimum, M_H as the value of $M(\varphi)$ at the minimum, and introducing the ultraviolet cutoff Λ_s one finds⁶⁻⁸ the following pattern of scales ($L = \ln(\Lambda_s/M_H)$)

$$\lambda \sim L^{-1} \quad m_h^2 \sim \langle\Phi\rangle^2 \cdot L^{-1} \quad M_H^2 \sim L \cdot m_h^2 = K^2 \langle\Phi\rangle^2 \quad (2)$$

K being a cutoff-independent constant. Furthermore, the relation $V_{\text{eff}}(\langle\Phi\rangle) \sim -M_H^4$ supports the cutoff independence of M_H , and therefore of $\langle\Phi\rangle$, because the ground state energy is a Renormalization Group invariant quantity, see.⁶⁻⁸

Notice that the two masses do not scale uniformly so that when $\Lambda_s \rightarrow \infty$ one would be left with only one mass, consistently with the free-field, continuum limit of the theory (“triviality”), see.⁸ Still, the two masses m_h and M_H refer to different momentum regions in the propagator ^a and could coexist in the cutoff theory.

^aThe zero-point energy is (one-half of) the trace of the logarithm of $G^{-1}(p)$. Therefore M_H , reflecting also the behaviour of the propagator at large Euclidean p^2 , in general differs from $m_h^2 \equiv |G^{-1}(p=0)|$.

As such, this two-mass structure was checked with lattice simulations of the propagator.⁶ Then, by computing m_h^2 from the $p \rightarrow 0$ limit of $G(p)$ and M_H^2 from its behaviour at higher p^2 , the lattice data are consistent with the scaling trend $M_H^2 \sim L m_h^2$ and in the full momentum region can be described by a model form⁸

$$G(p) \sim \frac{1 - I(p)}{2} \frac{1}{p^2 + m_h^2} + \frac{1 + I(p)}{2} \frac{1}{p^2 + M_H^2} \quad (3)$$

with an interpolating function $I(p)$ which depends on an intermediate momentum scale p_0 and tends to $+1$ for large $p^2 \gg p_0^2$ and to -1 when $p^2 \rightarrow 0$. Therefore the lattice data support the idea that, beside the known resonance with mass $m_h = 125$ GeV, the Higgs field might exhibit a second resonance with a much larger mass. At the same time, by extrapolating from various lattice sizes, the cutoff-independent constant was found $K = 2.80 \pm 0.04(\text{stat}) \pm 0.08(\text{sys})$ giving the prediction^{6–8}

$$(M_H)^{\text{Theor}} = 690 \pm 10 \text{ (stat)} \pm 20 \text{ (sys)} \text{ GeV} \quad (4)$$

The above numerical estimate, on the one hand, represents a definite prediction to compare with experiments. On the other hand, it helps to clarify the relation with the more conventional picture where there is only m_h . To this end, we note that, from the third relation in (2), one finds $m_h \ll M_H$ for very large Λ_s . But M_H is Λ_s -independent so that by decreasing Λ_s also the lower mass increases by approaching its maximum value $(m_h)^{\text{max}} \sim M_H$ for $L \sim 1$, i.e. when the cutoff Λ_s is a few times M_H . Therefore this maximum value corresponds to

$$(m_h)^{\text{max}} \sim (M_H)^{\text{Theor}} = 690 \pm 10 \text{ (stat)} \pm 20 \text{ (sys)} \text{ GeV} \quad (5)$$

in good agreement with the upper bound derived from the conventional first two relations in Eq.(2) $(m_h)^{\text{max}} = 670$ (80) GeV, see Lang's complete review.¹³ Equivalently, without performing our own lattice simulations of the propagator, we could have predicted $(M_H)^{\text{Theor}} = 670$ (80) GeV by combining the Λ_s -independence of M_H , the third relation in (2) and the estimate of $(m_h)^{\text{max}}$ in Lang's review paper. This means that for $\Lambda_s \rightarrow \infty$ the two masses decouple from each other while for $\Lambda_s = O(1)$ TeV the two masses coincide. However, the physical situation has $m_h = 125$ GeV so that, if M_H exists, Λ_s would be very large. At the same time, since vacuum stability would depend on the large M_H , and not on m_h , SSB could originate within the pure scalar sector regardless of the other parameters of the theory, e.g. the vector boson and top quark mass.

After this preliminary introduction, in this paper we will first briefly summarize in Sect.2 the expected phenomenology of the second resonance and then, in Sects.3, 4 and 5, argue that the existence of a new resonance in the predicted mass range find support in two analyses by ATLAS (searching for heavy resonances decaying into final states with 4 charged leptons or $\gamma\gamma$ pairs) and in more recent CMS results (searching for heavy resonances decaying into a pair of $h(125)$ bosons or looking for $\gamma\gamma$ pairs produced in pp double-diffractive scattering). Finally, Sect.6 will contain a summary and our conclusions.

2. Phenomenology of the second resonance

In spite of their substantial difference, the two masses m_h and M_H describe excitations of the *same* Higgs field. Therefore the observable interactions of this field, with itself and with the other fluctuations about the minimum of the potential, as the Goldstone bosons, are controlled by a single coupling: the mass parameter m_h^2 determining the boundary condition at the Fermi scale for the scalar coupling $\lambda = 3m_h^2/\langle\Phi\rangle^2$. Thus, in spite of its large mass, the H -resonance would couple to longitudinal W's and Z's with the same typical strength as the low-mass state ^b at 125 GeV and represent a relatively narrow resonance. This is illustrated by the replacement of the conventional large width for a heavy Higgs particle $\Gamma^{\text{conv}}(H \rightarrow WW + ZZ) \sim G_F M_H^3$ with the corresponding relation $\Gamma(H \rightarrow WW + ZZ) \sim M_H(G_F m_h^2)$ which defines the same phase-space factor M_H with a coupling re-scaled by the small ratio $m_h^2/M_H^2 \sim 0.032$. Numerically, for $M_H \sim 700$ GeV, from the results of ref.,¹⁷ this gives ^c

$$\Gamma(H \rightarrow ZZ) \sim \frac{M_H}{700 \text{ GeV}} \cdot \frac{m_h^2}{(700 \text{ GeV})^2} \quad 50.1 \text{ GeV} \sim \frac{M_H}{700 \text{ GeV}} \cdot 1.6 \text{ GeV} \quad (6)$$

$$\Gamma(H \rightarrow WW) \sim \frac{M_H}{700 \text{ GeV}} \cdot \frac{m_h^2}{(700 \text{ GeV})^2} \quad 102.6 \text{ GeV} \sim \frac{M_H}{700 \text{ GeV}} \cdot 3.3 \text{ GeV} \quad (7)$$

On the other hand, the decays into fermions, gluons, photons..., which are proportional to the gauge and yukawa couplings, would be unchanged and can be taken from¹⁷ yielding

$$\Gamma(H \rightarrow \text{fermions} + \text{gluons} + \text{photons}...) \sim \frac{M_H}{700 \text{ GeV}} \cdot 26.2 \text{ GeV} \quad (8)$$

Therefore, one might expect a total width $\Gamma_H \equiv \Gamma(H \rightarrow \text{all}) = 30 \div 31$ GeV. This estimate, however, does not account for the new contributions from the decays of the heavier resonance into the lower-mass state at 125 GeV. These include the two-body decay $H \rightarrow hh$, the three-body processes $H \rightarrow hhh$, $H \rightarrow hZZ$, $H \rightarrow hW^+W^-$ and the higher-multiplicity final states allowed by phase space. For this reason, the above value $30 \div 31$ GeV should only be considered as a lower bound.

It is not so simple to evaluate the new contributions to the total decay width because of the $h - H$ overlapping which makes this a non-perturbative problem. Perhaps, techniques as the RSE approach,¹⁴ used in analogous problems with meson resonances, could be useful. For this reason, in ref.,²¹ we considered a test in the

^bWe emphasize that the same result is also recovered in a unitary-gauge calculation of longitudinal W's scattering. There, at asymptotic energies and at the tree-level, the M_H^2 in the Higgs propagator is promoted to effective contact coupling $\lambda_0 = 3M_H^2/\langle\Phi\rangle^2$. But by re-summing higher-order terms with the β -function, at the Fermi scale one finds $\lambda_0 \rightarrow \lambda = 3m_h^2/\langle\Phi\rangle^2 \sim L^{-1}$, see⁸ and also.¹⁵

^cAs compared to the old values reported in,¹⁶ in the more recent ref.,¹⁷ there has been a substantial reduction of the conventional $G_F M_H^3$ decay widths into W's and Z's, from 56.7 and 115.2 GeV to 50.1 and 102.6 GeV respectively.

“golden” 4-lepton channel that does *not* require the knowledge of the total width but only relies on two assumptions:

- a) a resonant 4-lepton production through the chain $H \rightarrow ZZ \rightarrow 4l$
- b) the estimate of $\Gamma(H \rightarrow ZZ)$ in Eq.(6)

Therefore, by defining $\gamma_H = \Gamma_H/M_H$, we find a fraction

$$B(H \rightarrow ZZ) = \frac{\Gamma(H \rightarrow ZZ)}{\Gamma_H} \sim \frac{1}{\gamma_H} \cdot \frac{50.1}{700} \cdot \frac{m_h^2}{(700 \text{ GeV})^2} \quad (9)$$

that will be replaced in the cross section approximated by on-shell branching ratios

$$\sigma_R(pp \rightarrow H \rightarrow 4l) \sim \sigma(pp \rightarrow H) \cdot B(H \rightarrow ZZ) \cdot 4B^2(Z \rightarrow l^+l^-) \quad (10)$$

This should be a good approximation for a relatively narrow resonance so that one predicts a particular correlation

$$\gamma_H \cdot \sigma_R(pp \rightarrow H \rightarrow 4l) \sim \sigma(pp \rightarrow H) \cdot \frac{50.1}{700} \cdot \frac{m_h^2}{(700 \text{ GeV})^2} \cdot 4B^2(Z \rightarrow l^+l^-) \quad (11)$$

which can be compared with the LHC data.

Since $4B^2(Z \rightarrow l^+l^-) \sim 0.0045$, to check our picture, the only missing piece is the production cross section $\sigma(pp \rightarrow H)$ which, as discussed in,⁸ will mainly proceed through the gluon-gluon Fusion (ggF) process. In fact, production through Vector-Boson Fusion (VBF) plays no role once the large coupling to longitudinal W's and Z's is suppressed by the small factor $m_h^2/M_H^2 \sim 0.032$. Therefore, the sizeable VBF cross section $\sigma^{\text{VBF}}(pp \rightarrow H) \sim 300$ fb is reduced to about 10 fb and is negligible with respect to the pure ggF contribution $\mathcal{O}(10^3)$ fb. Indeed, for 13 TeV pp collisions, and with a typical $\pm 15\%$ uncertainty (due to the parton distributions, to the choice of μ in $\alpha_s(\mu)$ and to other effects), from ref.¹⁸ we find a value $\sigma^{\text{ggF}}(pp \rightarrow H) = 1090(170)$ fb which also accounts for the range $M_H = 660 \div 700$ GeV,

In conclusion, for $m_h = 125$ GeV, we obtain a sharp prediction which, for not too large γ_H where Eq.(10) loses validity, is formally insensitive to the value of Γ_H and can be compared with future high-precision 4-lepton data^d

$$[\gamma_H \cdot \sigma_R(pp \rightarrow H \rightarrow 4l)]^{\text{theor}} \sim (0.011 \pm 0.002) \text{ fb} \quad (12)$$

3. The ATLAS ggF-like 4-lepton events

To obtain indications on a possible new resonance around 700 GeV, we started from the ‘golden’ 4-lepton channel by considering the ATLAS sample^{19,20} of events that, for their typical characteristics, admit the interpretation of being produced through the ggF mechanism.

For these 4-lepton data, the ATLAS experiment has performed a multivariate analysis (MVA) which combines a multilayer perceptron (MLP) and one or two

^dThe 12% reduction of the $\Gamma(H \rightarrow ZZ)$ decay width, from 56.7 to 50.1 GeV,¹⁷ together with most recent estimate of the cross section $\sigma^{\text{ggF}}(pp \rightarrow H) = 1090(170)$ fb, has produced a sizeable reduction with respect to the value 0.0137(21) fb of ref.²¹

recurrent neural networks (rNN). The outputs of the MLP and rNN(s) are concatenated so as to produce an event score. In this way, depending on the score, the ggF events are divided into four mutually exclusive categories: ggF-MVA-high-4 μ , ggF-MVA-high- 2e2 μ , ggF-MVA-high-4e, ggF-MVA-low.

This class of ggF-like events was already considered in ref.²¹ with the conclusion that there are definite indications for a new resonance in the expected mass region. However, due to some model-dependent assumptions in the analysis of the data, here we have decided to adopt a different strategy. The starting point was to consider the other ATLAS article on the differential cross section, as function of the 4-lepton invariant mass,²² and in particular their Fig.5. The figure indicates a sizeable excess of events around 680 GeV which, soon after, is followed by a corresponding sizeable defect. Notice that the bins used at high masses have size of 60 GeV or more, probably to minimize smearing effects due to the invariant mass resolutions of the different final states. Indeed, for a 700 GeV resonance, the resolutions in invariant mass for 4e, 2e2 μ and 4 μ final states are approximately 12 GeV, 19 GeV and 24 GeV respectively²³ so that a bin of 60 GeV, centered at a given value with ± 30 GeV range, is large enough not to be significantly affected by smearing effects (with spurious migrations of events between neighboring bins).

By expecting our second resonance to be produced through gluon-gluon fusion (ggF) we then looked for indications in that particular sector and considered the category of the ggF-low events, which are homogeneous from the point of view of the selection and have sufficient statistics. At the same time, since this category contains a mixture of all three final states, it is natural to follow the above large-bin strategy. In our understanding, the ggF-low sample is certainly less pure as compared to the ggF-high samples, and it is true that it includes the dominating contribution from non-resonant ZZ events. On the other hand, according to ATLAS, this total background was carefully evaluated with a quoted total (stat. + syst.) uncertainty which is rather small (less than 5% in the relevant region²⁰). As such, we see no reason not to consider it as our best estimate and safely subtract the background from the observed events. The result of this subtraction is shown in Table 1.

From our Table 1, one gets the same qualitative impression as from Fig.5 of ref.²² in the same energy region. Namely, a sizeable (2.5-sigma) excess of events over the background, in the bin centered around 680 GeV, followed by a sizeable opposite defect (about 3-sigma) in the bin centered around 740 GeV. The simplest explanation for these two simultaneous features would be the existence of a resonance of mass $M_H \sim 700$ GeV which, beside the resonant peak, by interfering with the non-resonating background produces the characteristic change of sign of the interference term proportional to $(M_H^2 - s)$.

We have thus attempted to describe the data in Table 1 by using the same model

Table 1. For luminosity 139 fb^{-1} , we report the observed ATLAS ggF-low events and the corresponding estimated background²⁰ in the range of invariant mass $M_{4l} = E = 530 \div 830 \text{ GeV}$. To avoid spurious fluctuations, due to migration of events between neighbouring bins, we have followed the same criterion as in Fig.5 of ref²² by grouping the data into larger bins of 60 GeV , centered at $560, 620, 680, 740$ and 800 GeV . These were obtained by combining the corresponding 10 bins of 30 GeV , centered respectively at the neighbouring pairs: $545(15) \div 575(15) \text{ GeV}$, $605(15) \div 635(15) \text{ GeV}$, $665(15) \div 695(15)$, $725(15) \div 755(15) \text{ GeV}$ and $785(15) \div 815(15) \text{ GeV}$ as reported in ref.²⁰ In this energy range, the errors in the background are below 5% and will be ignored.

| E[GeV] | $N_{\text{EXP}}(E)$ | $N_{\text{bkg}}(E)$ | $N_{\text{EXP}}(E) - N_{\text{bkg}}(E)$ |
|---------|---------------------|---------------------|---|
| 560(30) | 38 ± 6.16 | 32.0 | 6.00 ± 6.16 |
| 620(30) | 25 ± 5.00 | 20.0 | 5.00 ± 5.00 |
| 680(30) | 26 ± 5.10 | 13.04 | 12.96 ± 5.10 |
| 740(30) | 3 ± 1.73 | 8.71 | -5.71 ± 1.73 |
| 800(30) | 7 ± 2.64 | 5.97 | 1.03 ± 2.64 |

cross section adopted in^{8,21}

$$\sigma_T = \sigma_B + \frac{2(M_H^2 - s) \Gamma_H M_H}{(s - M_H^2)^2 + (\Gamma_H M_H)^2} \sqrt{\sigma_B \sigma_R} + \frac{(\Gamma_H M_H)^2}{(s - M_H^2)^2 + (\Gamma_H M_H)^2} \sigma_R \quad (13)$$

which, together with the mass M_H and total width Γ_H of the resonance, introduces a background cross section $\sigma_B = \sigma_B(E)$ and a peak cross section σ_R . Of course, due to the very large size of the bins, ours should only be considered a first, rough approximation. Nevertheless, we found a good consistency with the phenomenological picture of Sect.2.

For our comparison, we first searched for an accurate description of the ATLAS background in terms of a power law $N_B(E) \sim A \cdot (710 \text{ GeV}/E)^\nu$ with $A \sim 10.55$ and $\nu \sim 4.72$. Then, by simple redefinitions, the theoretical number of events can be expressed as

$$N_{TH}(E) = N_B(E) + \frac{P^2 + 2P \cdot x(E) \cdot \sqrt{N_B(E)}}{\gamma_H^2 + x^2(E)} \quad (14)$$

where $x(E) = (M_H^2 - E^2)/M_H^2$, and P is defined as $P \equiv \gamma_H \sqrt{N_R}$ in terms of the extra number of events at the resonance peak $N_R = \sigma_R \cdot \mathcal{A} \cdot 139 \text{ fb}^{-1}$ for given acceptance \mathcal{A} and luminosity. Without a specific information on the acceptance of the ggF-low category, we adopted a value $\mathcal{A} \sim 0.38$ by averaging the two extremes, 0.30 and 0.46, quoted for the lowest and highest mass regions.¹⁹ As a consequence, the resonance parameters will be affected by a corresponding uncertainty. We then fitted with Eq.(14) the experimental number of events in Table 1. The results were: $M_H = 706(25) \text{ GeV}$, $\gamma_H = 0.041 \pm 0.029$ (corresponding to a total width $\Gamma_H = 29 \pm 20 \text{ GeV}$) and $P = 0.14 \pm 0.07$. From these we obtain central values $\langle N_R \rangle \sim 12$

and $\langle \sigma_R \rangle \sim 0.23$ fb with very large errors. Our theoretical values are shown in Table 2 and a graphical comparison in Fig.1.

Table 2. The experimental ATLAS ggF-low events are compared with our theoretical prediction Eq.(14) for $M_H = 706$ GeV, $\gamma_H = 0.041$, $P = 0.14$.

| E[GeV] | $N_{\text{EXP}}(E)$ | $N_{\text{TH}}(E)$ | χ^2 |
|---------|---------------------|--------------------|----------|
| 560(30) | 38 ± 6.16 | 36.72 | 0.04 |
| 620(30) | 25 ± 5.00 | 25.66 | 0.02 |
| 680(30) | 26 ± 5.10 | 26.32 | 0.00 |
| 740(30) | 3 ± 1.73 | 3.23 | 0.02 |
| 800(30) | 7 ± 2.64 | 3.87 | 1.40 |

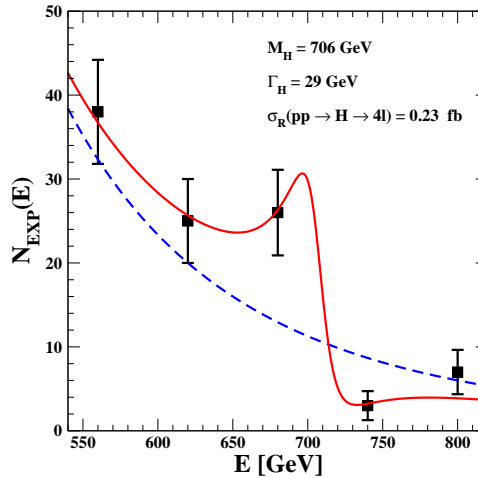


Fig. 1. The observed ATLAS ggF-low events are compared with Eq.(14) (the red continuous line) for resonance parameters $M_H = 706$ GeV, $\gamma_H = 0.041$ and peak cross section $\sigma_R = 0.23$ fb (equivalent to $P = 0.14$ and $N_R \sim 12$). The dashed blue line models ATLAS background as $N_B(E) \sim A \cdot (710 \text{ GeV}/E)^\nu$ with $A \sim 10.55$ and $\nu \sim 4.72$.

The quality of our fit is good but, with the exception of the mass, errors are very large and the test of our picture is not so stringent. Still, with the partial width of Sect.2, $\Gamma(H \rightarrow ZZ) \sim 1.6$ GeV, and fixing Γ_H to its central value of 29 GeV, we find a branching ratio $B(H \rightarrow ZZ) \sim 0.055$ which, for the central value $\sigma^{\text{ggF}}(pp \rightarrow H) \sim 923$ fb¹⁷ at $M_H = 700$ GeV, would imply a theoretical peak cross section $(\sigma_R)^{\text{theor}} = (923 \cdot 0.055 \cdot 0.0045) \sim 0.23$ fb which coincides with the central value from our fit. Also, from the central values of our fits $\langle \sigma_R \rangle = 0.23$ fb and $\langle \gamma_H \rangle = 0.041$ we find $\langle \sigma_R \rangle \cdot \langle \gamma_H \rangle \sim 0.0093$ fb consistently with the theoretical prediction Eq.(12).

In conclusion, the ATLAS ggF-low category of 4-lepton events indicate the existence of a new resonance whose mass and basic parameters are consistent with our picture.

4. The ATLAS high-mass $\gamma\gamma$ events

Looking for further signals, we have then considered the ATLAS $\gamma\gamma$ events in the range of invariant mass $600 \div 770$ GeV which extends about ± 90 GeV around our central mass value. The relevant entries in Table 3 were extracted from Fig.3 of²⁴ because the numerical values are not reported in the companion HEPData file.

Again, we have performed various fits to the corresponding cross sections by parameterizing the background with a power-law form $\sigma_B(E) \sim A \cdot (685 \text{ GeV}/E)^\nu$. This gives a good description of all data, with the exception of the sizeable excess at 684 GeV (estimated by ATLAS to have a local significance of about 3.3-sigma). To have an idea, by fixing $\sigma_R = 0$ in Eq.(13), a pure background fit gives $A = 1.35(3)$ fb and $\nu = 4.87(38)$ with $\chi^2 = 14$, but 10 of which are only due to the peak at 684 GeV, see Fig.2.

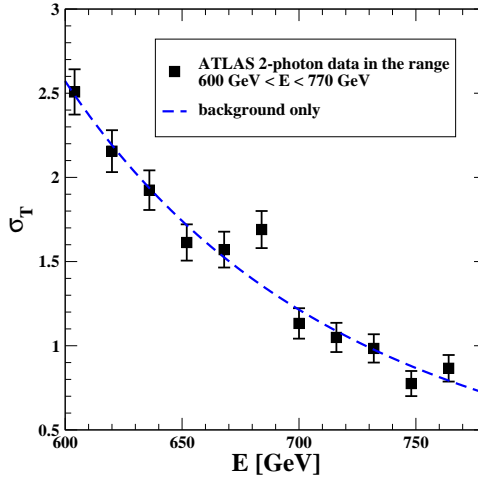


Fig. 2. The fit with Eq.(13) and $\sigma_R = 0$ to the data in Table 2, transformed into cross-sections in fb. The chi-square value is $\chi^2 = 14$ and the background parameters $A = 1.35$ fb and $\nu = 4.87$.

Therefore the (hypothetical) new resonance might remain hidden by the large background almost everywhere, the main signal being just the interference effect. However, since this interference effect is much smaller than the background in the resonance region ($\sigma_B \sim 1.3$ fb), the resonance parameters will be determined very poorly. In this perspective, our scope is not to provide a better-quality fit but to show that the same $\gamma\gamma$ data are also well consistent with the existence of a new resonance in the expected mass region.

To this end, by constraining the background parameters A and ν in σ_B to lie within the region from the previous fit for $\sigma_R = 0$, we have performed several fits with the full Eq.(13). Three fits are shown in Fig.3 for $M_H = 696$ GeV and for the values $\Gamma_H = 20, 30$ and 40 GeV.

Table 3. We report the ATLAS number of $N = N(\gamma\gamma)$ events, in bins of 16 GeV and for luminosity 139 fb^{-1} , for the range of invariant mass $\mu = \mu(\gamma\gamma) = 600 \div 770$ GeV. These entries were directly extracted from Fig.3 of²⁴ because the relevant numbers are not reported in the corresponding HEPData file.

| μ | 604 | 620 | 636 | 652 | 668 | 684 | 700 | 716 | 732 | 748 | 764 |
|-------|---------|---------|---------|---------|---------|---------|---------|---------|---------|---------|---------|
| N | 349(19) | 300(17) | 267(16) | 224(15) | 218(15) | 235(15) | 157(13) | 146(12) | 137(12) | 108(10) | 120(11) |

Due to the predominant role of the interference effect, in this $\gamma\gamma$ case, we also did a second series of fits by reversing the sign of the interference term (from positive to negative below peak) which is not known a priori. For the same values of the width reported in Fig.3, the corresponding fits are shown in Fig.4. Note that, in this second type of fits there is a shift of about -30 GeV, in the central value of the mass, from $M_H = 696(12)$ GeV down to $M_H = 665(13)$ GeV.

Thus, in principle, the localized 3.3-sigma excess at 684 GeV admits two different interpretations:

- a) a statistical fluctuation above a pure background, see fit in Fig.2
- b) the signal of a new resonance, see Figs.3 and 4

As for the total width, the $\gamma\gamma$ data tend to place an upper limit which could be summarized as $(\Gamma_H)^{\text{exp}} < 50$ GeV. The analogous combined determination for the mass could be summarized into $(M_H)^{\text{exp}} = 680(15)$ GeV which summarizes the results obtained with the two possible signs of the interference term in Eq.(13).

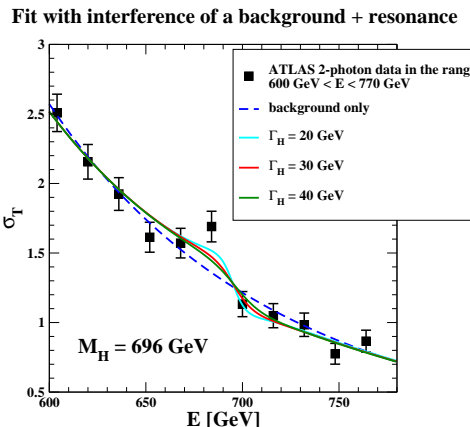


Fig. 3. Three fits with Eq.(13) to the data in Table 2, transformed into cross-sections in fb. The χ^2 -values are 8.0, 9.5, 10.7 respectively for $\Gamma_H = 20, 30$ and 40 GeV.

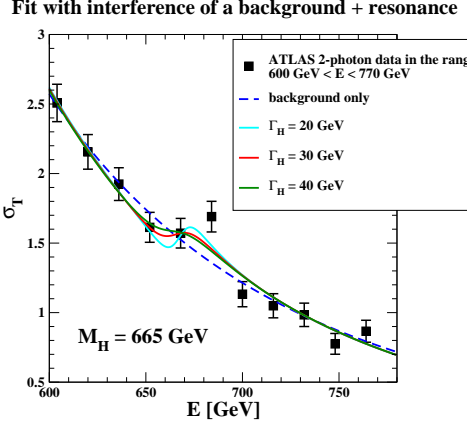


Fig. 4. Three fits with Eq.(13) to the data in Table 2, transformed into cross-sections in fb. With respect to Fig.3, we have reversed the sign of the interference term in Eq.(13). The χ^2 -values are 9.6, 10.4 and 11.0 respectively for $\Gamma_H = 20, 30$ and 40 GeV.

As for the peak cross section $\sigma_R = \sigma_R(pp \rightarrow H \rightarrow \gamma\gamma)$, its values are always very small. The central values lie in the range $0.004 \div 0.009$ fb with minus errors, however, which, at the 70% confidence level, extend very close to $\sigma_R \sim 0$ (where $\chi^2 = 14$). Therefore, before concluding this section, it is appropriate to comment on the theoretical prediction for this quantity which depends on the partial width $\Gamma(H \rightarrow \gamma\gamma)$.

For the definite value $M_H = 700$ GeV, the estimate of ref.¹⁷ is $\Gamma(H \rightarrow \gamma\gamma) = 29$ keV. Therefore, for $(\Gamma_H)^{\text{Exp}} = 30 \div 40$ GeV, one might expect a branching ratio $B(H \rightarrow \gamma\gamma) \sim 8 \cdot 10^{-7}$ and a peak cross section $\sigma_R(pp \rightarrow H \rightarrow \gamma\gamma) \sim \sigma(pp \rightarrow H) \cdot B(H \rightarrow \gamma\gamma) \sim 8 \cdot 10^{-4}$ fb. However, it should be emphasized that this estimate of $\Gamma(H \rightarrow \gamma\gamma)$ contains the non-decoupling, so called, “-2” term proportional to M_H^3 whose existence (or not) in the WW contribution has been discussed at length in the literature. At present, the general consensus is that this term has to be there with the only exception of the unitary-gauge calculations of Gastmans, Wu and Wu²⁵⁻²⁷ and the dispersion-relation approach of Christova and Todorov.²⁸ We believe that, in the context of a second Higgs resonance, which does *not* couple to longitudinal W's proportionally to its mass but with the same typical strength as the low-mass state at 125 GeV, the whole issue could be re-considered. The point is that for the range of mass around $M_H = 700$ GeV there are strong cancellations between the WW and $t\bar{t}$ contributions. As we have checked, the presence or not of the non-decoupling term could easily change the lowest-order value (i.e. without QCD corrections in the top-quark graphs) by an order of magnitude. For this reason, an increase of the partial decay width up to $\Gamma(H \rightarrow \gamma\gamma) \lesssim 100$ keV cannot be excluded. This would increase the theoretical branching ratio and, therefore, the theoretical peak cross section toward the region $\sigma_R(pp \rightarrow H \rightarrow \gamma\gamma) = O(10^{-3})$ fb favoured by our fit to the $\gamma\gamma$ events.

Of course, more precise data are needed for a significative test. However since, most probably, even with the whole integrated luminosity from RUN3, the statistical errors will not change substantially, one could search for additional information from other channels. For instance, from $\gamma\gamma$ exclusive production in pp double-diffractive scattering, i.e. in the process

$$p + p \rightarrow p + X + p \quad (15)$$

when both final protons are tagged and have large Feynman x_F . For $X = H$, which is the “diffractive excitation of the vacuum” considered by Albrow,³⁴ one could then look for an excess of $\gamma\gamma$ events in the region of invariant mass $\mu(\gamma\gamma) \sim M_H$. Since, here, the background is different, the corresponding excess could have a larger statistical significance. Remarkably, as we will briefly discuss in the following section, such an excess is indeed present in the CMS data.

5. Experimental signals from CMS: a survey

Unfortunately CMS analyses of charged 4-lepton and fully inclusive photon pair events, with the whole statistics collected during RUN2, are not yet available. However, we report below some indications from smaller statistical samples to get, at least, the qualitative indication of some excess in the relevant mass region.

In this respect, the CMS 35.9 fb^{-1} 4-lepton data show a clean excess around 660 GeV (see Fig.3, left panel of²⁹), consistently with the corresponding ATLAS sample with the full 139 fb^{-1} luminosity. This is also visible in first panel (up left) of Fig.2 of³⁰ with the same clean statistical significance.

The corresponding $\gamma\gamma$ data, for the same statistics of 35.9 fb^{-1} , also show a modest 1-sigma excess for the EBEB selection mode, see Fig.2, left panel of.³¹ The data were grouped into bins of 20 GeV and the relevant concerns the three bins from 620(10) to 660(10) GeV. The analogous EBEE plot also shows a very slight excess at 660 GeV but this is really too small. The 1-sigma excess for 640(30) GeV in the EBEB is also visible in panel 5 of Fig.4 of³¹ where the data are compared with the case of a scalar resonance, for $\gamma_H = 0.056$ which is close to our model. Notice that the excess is followed by a corresponding defect of events as in the ATLAS 4-lepton case we have discussed. The corresponding plot in panel 6 for the EBEE mode shows instead only a defect of events.

While, to present date, there is no CMS analysis of high-mass $\gamma\gamma$ pairs with a statistics larger than 35.9 fb^{-1} , high-mass, 4-lepton events with the larger 77.4 fb^{-1} luminosity were reported in.³² Though, it is very hard to deduce anything from the very compressed scale adopted for the figures (see however Cea’s analysis³³ claiming for a substantial excess around 700 GeV). From this point of view, these partial CMS measurements certainly do not contradict our present analysis.

But a second resonance of the Higgs field, if there, should also be visible in other decay channels as well. For this reason, we will now discuss some results presented by CMS at the ICHEP 2022 Conference and/or made recently publicly accessible. A

first analysis³⁵ concerns the search for high mass resonances decaying into W-pairs which then decay into neutrinos and the charged leptonic final state ($e\mu$, $\mu\mu$, ee). The excesses observed have non-negligible local significances which range from 2.6 to 3.8 sigmas, depending on the different mechanisms for the resonance production mode (ggF and/or VBF). The scenario with $VBF = 0$ has the maximal significance for a resonance of mass 950 GeV, however, the region where one can see a deviation above 1 sigma is quite broad, 600 - 1200 GeV, due to the presence of neutrinos in the final state, and this is consistent with an excess in a mass region that also includes the one we predicted.

Another analysis³⁶ concerns the search for new resonances decaying, through two intermediate scalars, into the peculiar final state made by a $b\bar{b}$ quark pair and a $\gamma\gamma$ pair. In particular, here one has been considering the cross section for the full process

$$\sigma(\text{full}) = \sigma(pp \rightarrow H \rightarrow hh \rightarrow b\bar{b} + \gamma\gamma) \quad (16)$$

(in the CMS paper the new heavy resonance is called X and the 125 GeV resonance is called H while here we denote $X \equiv H$ and define $h = h(125)$). For a spin-zero resonance, the 95% upper limit $\sigma(\text{full}) < 0.16$ fb, for invariant mass of 600 GeV, was found to increase by about a factor of two, up to $\sigma(\text{full}) < 0.30$ fb in a plateau 650 \div 700 GeV, and then to decrease for larger energies. The local statistical significance is modest, about 1.6-sigma, but the relevant mass region 675(25) GeV is precise and agrees well with our analysis of the ATLAS data. Interestingly, if the cross section is approximated as

$$\sigma(\text{full}) \sim \sigma(gg \rightarrow H) \cdot B(H \rightarrow hh) \cdot 2 \cdot B(h \rightarrow b\bar{b}) B(h \rightarrow \gamma\gamma) \quad (17)$$

after replacing our reference value $\sigma(gg \rightarrow H) = 1090(170)$ fb, $B(h \rightarrow b\bar{b}) \sim 0.57$ and $B(h \rightarrow \gamma\gamma) \sim 0.002$, the CMS 95% upper bound $\sigma(\text{full}) < 0.30$ fb gives a rather precise upper bound $B(H \rightarrow hh) < 0.12$. In view of the mentioned non-perturbative nature of the decay process $H \rightarrow hh$ this represents a precious indication.

Finally, as anticipated, CMS has been searching for high-mass photon-pairs exclusively produced in pp diffractive scattering, i.e. when both final protons have large x_F . For our scopes, the relevant information is contained in Fig.5, fourth panel (second row, right) of.³⁷ In the range of invariant mass 650(40) GeV, and for a statistics of 102.7 fb^{-1} the observed number of $\gamma\gamma$ events was $N_{\text{obs}} \sim 76(9)$ to be compared with an estimated background $N_{\text{BKG}} \sim 40(6)$. In the most conservative case, this is a local excess of 3.3-sigma significance.

Now, our understanding is that the uncertainty on the background of each bin has been evaluated by means of high-statistics samples which account for the most important processes ($t\bar{t}$ +jet; $Z + \gamma$, $W + \gamma$; $\gamma +$ jet; QCD events) fully simulated in the detector, reconstructed as the real data and subjected to the same type of analysis as the real data. For the relevant bin with invariant mass 650(40) GeV, this sophisticated procedure gives a background estimate of 40 events with an uncertainty of ± 6 described by the hatched area in the plot of Fig.5, fourth panel

(second row, right) of,³⁷ see also the lower part for the ratio Data/Prediction. As one can see, apart from two points with large errors around 1 TeV, all bins lie within the hatched area, *except* the bin at 650(40)GeV where the 76(9) observed events correspond indeed to the mentioned 3.3-sigma excess. However, a critical observer cannot help but notice that interpolating the background yields from the two neighbouring bins would suggest a background estimate which is closer to 60 rather than 40. Starting from this remark, within the CMS Collaboration, an effort should be made to see whether, in the end, with a more refined evaluation of the background (and adding the remaining statistics of about 35 fb^{-1} events) the excess will maintain the present, sizeable statistical significance.

At present, the two excesses found in the two previous CMS analyses point to a new resonance of mass $(M_H)^{\text{Exp}} \sim 670(20)$ GeV.

6. Summary and conclusions

In this paper, we started from the idea^{6–8} that, beside the known resonance with mass $m_h = 125$ GeV, the Higgs field could exhibit a second resonance with a much larger mass M_H . This new state, however, would couple to longitudinal W's with the same typical strength as the low-mass state at 125 GeV and thus represent a relatively narrow resonance mainly produced at LHC by gluon-gluon fusion (ggF). From theoretical arguments and lattice simulations, its mass can be estimated to have a value $(M_H)^{\text{Theor}} = 690 \pm 10$ (stat) ± 20 (sys) GeV.

To find some signal in the LHC data, we started in Sect.3 with the ATLAS search for a new resonance in the charged 4-lepton channel by considering the ggF-low category of events which forms a homogeneous sample and has sufficient statistics. As reported in Table 1, this sample shows a 2.5-sigma excess at 680(30) GeV followed by an opposite 3-sigma deficit at 740(30) GeV. This feature is also confirmed by Fig.5 of.²² As we have argued, the simplest explanation would be the existence of a new resonance with mass $M_H \sim 700$ GeV which, besides the Breit-Wigner peak, produces the characteristic $(M_H^2 - s)$ interference effect. As shown in Table 2 and in Fig.1, this interpretation is consistent with the data for the range of parameters suggested by the phenomenological picture of Sect.2.

After this first indication, we have considered in Sect.4 the ATLAS $\gamma\gamma$ events in the high-mass region $600 \div 770$ GeV. As we have shown, see Figs.2-4, the sizeable 3.3-sigma (local) excess at 684 GeV in the $\gamma\gamma$ distribution can also be interpreted as the interference signal, with a dominating background, of a new resonance whose mass $(M_H)^{\text{exp}} \sim 680(15)$ GeV is again in the expected mass range. As for the total width, the $\gamma\gamma$ data tend to place an upper limit $(\Gamma_H)^{\text{exp}} < 50$ GeV (consistently with the very loose indication $(\Gamma_H)^{\text{exp}} = 29(20)$ GeV from the 4-lepton sample).

Since the analogous CMS full distributions, for the high-mass 4-lepton and inclusive $\gamma\gamma$ events, are still missing, we first considered in Sect.5 previous CMS small-sized samples for these two channels. The lower statistics results do not contradict the existence of a new resonance in the relevant mass region but do not add

much to the discussion, We thus considered two more recent CMS analyses which indicate a modest 1.6-sigma (local) excess at 675(25) GeV in the $b\bar{b} + \gamma\gamma$ final state and a sizeable 3.3-sigma (local) excess at 650(40) GeV in the invariant mass of $\gamma\gamma$ pairs produced in pp double-diffractive scattering. Altogether, these two CMS results point toward a new resonance with a mass of about 670(20) GeV.

In view of the good agreement with the indications extracted from the ATLAS data, it is natural to wonder about the present, overall statistical significance. To this end, one should first take into account that, when comparing with some theoretical prediction which refers to a definite mass region, as in the case of Eq.(4), local excesses should maintain intact their statistical significance and *not* be downgraded by the so called look-elsewhere effect.

For this reason, since the correlation among the above measurements is presumably very small and all effects are concentrated in the same mass region (the 2.5-sigma excess at 680(30) GeV followed by the 3-sigma defect at 740(30) GeV in the ATLAS 4-lepton channel, the 3.3-sigma excess at 684(8) GeV in the ATLAS $\gamma\gamma$ channel, the 1.6-sigma excess at 675(25) GeV in the CMS $b\bar{b} + \gamma\gamma$ final state and the 3.3-sigma excess at 650(40) GeV in the CMS diphoton events produced in pp double-diffractive scattering) one may observe that the cumulated statistical significance has reached a substantial level. Indeed, there are several, completely different analyses, done by two different experiments, that, in spite of not having been optimized for the kind of resonance we have predicted, show excesses of events exactly in the mass region of our interest.

Still, there is no question, announcing a discovery would be too premature for, at least, two reasons.

First, we have only taken into account the intrinsic \sqrt{N} statistical errors and neglected the systematic uncertainties which are needed in an experimental analysis claiming that something new has been discovered. In particular this remark is true for a typical Higgs search at LHC which has thousands of nuisance parameters that are determined together with the physical parameters of interest. As a definite example of systematic uncertainty, we have considered in Sect.5 the 3.3-sigma excess at 650(40) GeV in the invariant mass of diphoton events produced in pp double-diffractive scattering, but exactly the same discussion could be repeated for the other effects. In the end, after a more careful re-evaluation of all backgrounds and by increasing the statistics, the cumulated significance could be considerably weakened with respect to the present sizeable level.

Second, there are other final states which, at present, show no appreciable difference from the estimated background. While this represents a general warning, it is not a good reason to ignore the indications we have brought to the attention of the reader. Actually, it is just the opposite because, given the present energy and luminosity of LHC, the hypothetical second resonance is too heavy to be immediately seen in all possible final states. Instead, the existence of deviations, in some channel and in a particular energy range, should give motivations to sharpen the analysis in the other sectors.

With all possible caveats, we thus conclude, this intriguing situation could be definitely clarified when two crucial pieces of information which are still missing will be available: the final RUN2 high-mass distributions for the charged 4-lepton channel and for the inclusive $\gamma\gamma$ final state of the CMS Collaboration, possibly including this time a dedicated study to prove or disprove our prediction.

References

1. M. Tanabashi et al. (Particle Data Group), Phys. Rev. D **98** (2018) 030001.
2. P.H. Lundow, K. Markström, Physical Review E **80** (2009) 031104.
3. P.H. Lundow, K. Markström, Nucl. Phys. B **845** (2011) 120.
4. S. Akiyama, et al., Phys. Rev. D **100** (2019) 054510.
5. S.R. Coleman, E.J. Weinberg, Phys. Rev. D **7** (1973) 1888.
6. M. Consoli, L. Cosmai, Int. J. Mod. Phys. A **35** (2020) 2050103, hep-ph/2006.15378.
7. M. Consoli, L. Cosmai, Symmetry **12**, 2020, 2037; doi:10.3390/sym12122037.
8. M. Consoli, Contribution to Veltman Memorial Volume, Acta Phys. Pol. B **52** (2021) 763; arXiv: 2106.06543 [hep-ph].
9. M. Consoli, P.M. Stevenson, Int. J. Mod. Phys. A **15** (2000) 133, hep-ph/9905427.
10. P. M. Stevenson, Phys. Rev. D **32** (1985) 1389.
11. I. Stancu and P. M. Stevenson, Phys. Rev. D **42** (1990) 2710.
12. P. Cea, L. Tedesco, Phys. Rev. D **55** (1997) 4967.
13. C. B. Lang, "Computer Stochastics in Scalar Quantum Field Theory", Proceedings of NATO Advanced Study Institute on Stochastic Analysis and Applications in Physics, p. 133, Springer Science+Business Media, 1993, arXiv:hep-lat/9312004.
14. E. van Beveren, G. Rupp, Mod. Phys. Lett. A **19**, 1949 (2004).
15. P. Castorina, M. Consoli and D. Zappalà, J. Phys. G **35**, 075010 (2008); arXiv:0710.0458 [hep-ph].
16. Report of the LHC Higgs Cross Section Working Group; S. Dittmaier, et al. Eds., arXiv:1101.0593 [hep-ph].
17. BSM Higgs production cross sections at $\sqrt{s}=13$ TeV (update in CERN Report4 2016) /twiki.cern.ch/twiki/bin/view/LHCPhysics/CERNYellowReportPageBSMAAt13TeV
18. <https://twiki.cern.ch/twiki/bin/view/LHCPhysics/CERNYellowReportPageAt13TeV>.
19. ATLAS Collaboration, Eur. Phys. J. C **81** (2021) 332, arXiv:2009.14791 [hep-ex],
20. <https://www.hepdata.net/record/ins1820316>.
21. M. Consoli, L. Cosmai, Int. J. Mod. Phys. A **37**, (2022) 2250091; arXiv:2111.08962 v3 [hep-ph].
22. ATLAS Collaboration, JHEP **07** (2021) 005; arXiv:2103.01918v1 [hep-ex].
23. ATLAS Collaboration, Eur. Phys. J. C **78** (2018) 293.
24. ATLAS Collaboration, Phys. Lett. B **822**, 136651 (2021).
25. R. Gastmans, S. L. Wu and T. T. Wu, arXiv:1108.5322 [hep-ph].
26. S. L. Wu and T. T. Wu, Int. J. Mod. Phys. A **31** (2016) 1650028.
27. T. T. Wu and S. L. Wu, Nucl. Phys. B **914** (2017) 421.
28. E. Christova and I. Todorov, Bulg. J. Phys. **42** (2015) 296, arXiv:1410.7061.
29. CMS Collaboration, JHEP **11** (2017) 047.
30. CMS Collaboration, JHEP **06** (2018) 127.
31. CMS Collaboration, Phys. Rev. D **98** (2018) 092001.
32. CMS Collaboration, CMS PAS HIG-18-001
33. P. Cea, Mod. Phys. Lett. A **34** (2019) 1950137.

34. M. Albrow, “Double Pomeron Exchange: from the ISR to the LHC”, AIP Conf.Proc.1350:119-123,2011; arXiv:1010.0625 [hep-ex].
35. CMS Collaboration, CMS PAS HIG-20-016.
36. CMS Collaboration, CMS PAS HIG-21-011.
37. CMS and TOTEM Collaborations, CMS PAS EXO-21-007.